

# Improvements in the response calculation of the dual thin scintillator neutron detector

Mauro S. Dias

*Instituto de Pesquisas Energéticas e Nucleares – CNEN/SP, Caixa Postal 11049, São Paulo, Brazil*

Received 9 October 1991 and in revised form 30 March 1992

The present work describes the new features introduced in the Monte Carlo code – developed for efficiency and proton recoil spectra calculations of the dual thin scintillator (DTS) neutron detector – in order to achieve better accuracy and shorter processing time. The improvements include: relativistic kinematics, anisotropy in the angular distributions and application of the forced collision technique. The new calculated values are compared with experimental results at two neutron energies, namely: 2.446 and 14.04 MeV, obtained by means of the time correlated associated particle technique.

## 1. Introduction

In a previous paper [1] a Monte Carlo code has been described for efficiency and proton recoil spectra calculation of the dual thin scintillator (DTS) neutron detector [1–3]. At that time, the overall accuracy obtained in the calculation was between 1.4 and 2.1% for the 1–15 MeV energy range. As the accuracy in the  $H(n, n)H$  cross section improved substantially from the ENDF/B versions V to VI (1.0 to 0.3%), it became necessary to revise the Monte Carlo code in order to achieve better accuracy. At the same time weighting techniques were included in order to reduce the processing time. This allowed a higher number of histories to be followed, resulting in better statistics in the calculation.

## 2. General features of the Monte Carlo code

The detector parameters and the coordinate system orientation are shown in fig. 1. The detector is considered as a cylinder of height  $H_T$  and radius  $R$ , filled with scintillator containing hydrogen and carbon of concentrations  $N_H$  and  $N_C$ , respectively. The neutron beam, with a radius  $R_N$ , is assumed to be homogeneous and normally incident upon the detector front-face. Nonhomogeneity or other incidence angles may be easily introduced according to the case of interest.

The cylindrical regions where the scintillators 1 and 2 are located are called zones 1 and 2, respectively.

Zone 3 is located outside the scintillators. The contribution of the perspex light guide for the detector response was not considered. It has been estimated to be negligible for neutron beam diameters much smaller than the detector diameter [2]. Easy modifications can be introduced in the code to calculate the response for neutron beams comparable to or larger than the scintillators.

In the new version, a statistical uncertainty of around 0.4% can be achieved by applying the forced collision technique and running about  $10^5$  histories. Good pulse height distributions are obtained with  $4 \times 10^5$  histories.

## 3. Reaction cross sections and kinematics

Relativistic kinematics were applied for both  $H(n, n)H$  and  $C(n, n)C$  reactions. The equations were derived from the general formalism given in ref. [4].

In the case of  $H(n, n)H$  reaction, the elastic scattered neutron energy is given by:

$$E' = \frac{E}{2} [1 + \cos \theta'], \quad (1)$$

where  $E$  is the incident neutron energy and  $\theta'$  is the neutron scattering angle in the center-of-mass system. Eq. (1) can be used for both relativistic and nonrelativistic cases.

In the case of  $C(n, n)C$  reaction the code has the option of calculating the elastic scattered neutron en-

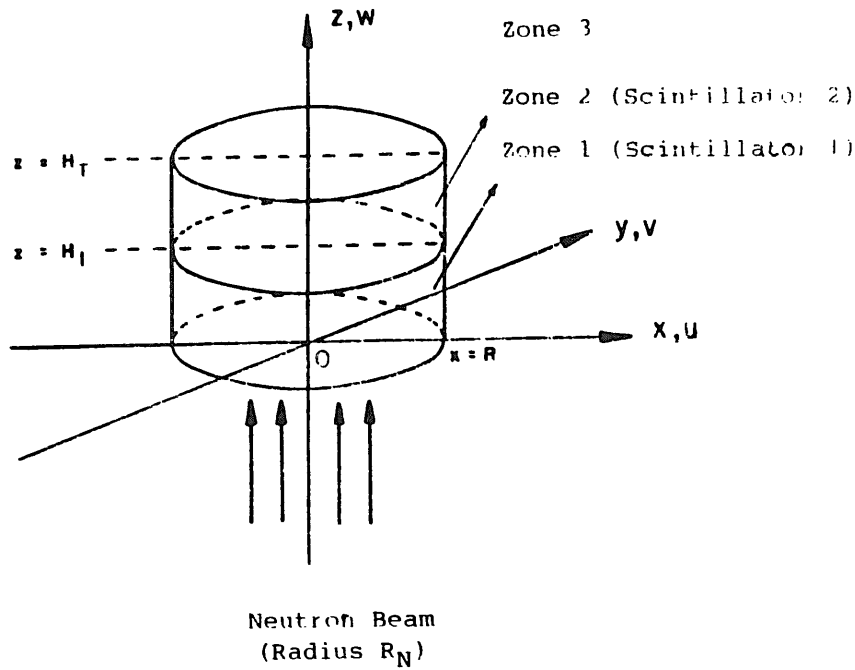


Fig. 1. Coordinate system. Zone 3 is the region outside the scintillators.

ergy relativistically by the following formula:

$$E' = \frac{E}{169} \left\{ 2 \left[ 1 + \frac{E}{2E_0} \right] \times \cos \theta \left[ \cos \theta + (\cos^2 \theta + 143)^{1/2} \right] + 143 \left[ 1 + \frac{E}{13E_0} \right] \right\} / \left\{ 1 + \frac{2E}{13E_0} \left[ 1 + \frac{E}{26E_0} \right] - 2 \frac{E}{169E_0} \left[ 1 + \frac{E}{2E_0} \right] \cos^2 \theta \right\}, \quad (2)$$

where  $E_0 = 939.573$  MeV is the neutron rest energy.

For the  $C(n, n'\gamma)C$  reaction the anisotropy in the angular distribution of scattered neutrons has been considered. The Legendre coefficients were taken from ref. [5] for the energy range between 8970 and 14930 keV. For the remaining energy range (between 4812 and 20000 keV) the coefficients were taken from the ENDF/B-V [6]. The selection of the scattering angle  $\theta$  has been performed similarly to the  $H(n, n)H$  case. For the accepted trial the energy of the inelastically scattered neutron was calculated in the center-of-mass system by the following nonrelativistic approximation:

$$E' = E \left[ \frac{145}{169} + \frac{156Q}{169E} + \frac{24}{169} \times \cos \theta' \left( 1 + \frac{13Q}{12E} \right)^{1/2} \right]. \quad (3)$$

After calculating  $E'$ , the scattering angle  $\theta'$  has been converted to the laboratory angle  $\theta$ :

$$\cos \theta = (1 + 12 \cos \theta' S_Q) / (145 + 144 S_Q^2 + 24 \cos \theta' S_Q)^{1/2}, \quad (4)$$

where  $S_Q = (1 + 13Q/12E)^{1/2}$ .

The detection of gamma-rays from the  $^{12}C(n, n'\gamma)^{12}C$  reaction has been calculated separately by means of a simplified Monte Carlo code as described in ref. [2]. The results of the correction factor due to this effect are shown in table 1 for a neutron beam

Table 1

Results of the correction factor due to the detection of gamma-rays from the  $^{12}C(n, n'\gamma)^{12}C$  reaction

Energy [keV]	Correction factor	Energy [keV]	Correction factor
4850	1.0000	6540	1.0025
4930	1.0003	6640	1.0017
4980	1.0005	7180	1.0015
5100	1.0004	8044	1.0037
5180	1.0004	9000	1.0022
5280	1.0009	10000	1.0024
5380	1.0014	11000	1.0024
5550	1.0012	12224	1.0014
5900	1.0019	13250	1.0012
6250	1.0025	14000	1.0010
6350	1.0031	14750	1.0008
6410	1.0024	15477	1.0007

Table 2  
 $^{12}\text{C}(n, n')3\alpha$  reaction  $Q$  values for different excitation levels of the  $(^{12}\text{C} + n)^*$  compound nucleus

Level index	$Q$ value [keV]	Level index	$Q$ value [keV]
1	7275	10	13250
2	7655	11	13750
3	9638	12	14250
4	10300	13	14750
5	10840	14	15250
6	11250	15	15750
7	11750	16	16250
8	12250	17	16750
9	12750	18	17250

incident on the detector axis. For finite neutron beam sizes the correction tends to be lower.

The  $Q$  value for the  $^{12}\text{C}(n, n')3\alpha$  reaction has been determined considering all the excitation energy levels, real or virtual, contained in the ENDF/B-V [6]. For each neutron energy a set of excitation probability values,  $P_i$ , has been generated for the compound nucleus states. This probability is the ratio between the partial cross section for a given excitation state and the total cross section for that neutron energy. These cross section values were also taken from ENDF/B-V. The excitation state is selected by comparing  $P_i$  with a random number  $R$  between [0,1]. If  $R < P_i$  the level is accepted and  $Q$  is given by the  $i$ th value in table 2.

#### 4. Application of the forced first collision technique

This technique allows a reduction in the number of histories followed by the Monte Carlo code, without significant loss in the achieved statistical accuracy. It was used to define the point where the first neutron collision will occur or to make the neutron collide preferentially with the hydrogen atoms in the scintillator.

Table 3 shows the percentage of contribution in the DTS detector efficiency from events originated by neu-

Table 3  
 Contribution to the DTS detection efficiency of events of originated by neutron first collision with hydrogen and carbon and in zones 1 and 2 (in percent)

Neutron energy [MeV]	Contribution to the efficiency [%]			
	Hydrogen	Carbon	Zone 1	Zone 2
1.0	89.0	11.0	95.6	4.4
2.4	93.8	6.2	96.7	3.3
14.0	96.4	3.6	98.6	1.4

tron first collision with hydrogen and carbon for different neutron energies. 89–96% of the contribution comes from events where the first neutron collision was with hydrogen.

Since the ratio between the total cross sections of hydrogen and carbon are in the range of 0.5 to 3, for 1 to 15 MeV neutrons, the fraction of neutrons which have first collision with hydrogen is between 30 and 77%. Therefore, it becomes convenient to force the first collision with hydrogen in order to reduce the processing time by a factor up to about 3.

A fraction  $f_H$  of the incident neutrons if forced to collide with hydrogen and  $(1 - f_H)$  collide with carbon atoms. The number of counts in the proton-recoil spectrum becomes a real number  $X$  given by

$$X = \begin{cases} 1 & \text{(hydrogen),} \\ \frac{f_H}{(1 - f_H)} \left( \frac{\Sigma_T}{\Sigma_H} - 1 \right) & \text{(carbon).} \end{cases} \quad (5)$$

The number of processed neutrons,  $N_s$ , gives rise to a larger number of counts in the proton-recoil spectrum,  $N'_s$ , given by

$$N'_s = f_H \frac{\Sigma_T}{\Sigma_H} N_s. \quad (6)$$

The processing time is reduced by the factor  $N'_s/N_s$ . At 14 MeV and using  $f_H = 0.9$ , this factor is equal to 2.4.

As shown in table 3, between 95 and 99% of the counts which contribute to the efficiency are originated by a neutron first collision in the first scintillator (Zone 1). Because of the high transmission through the detector for 1 to 15 MeV neutrons, about half of the neutrons are incident in zone 1 and half are incident in zone 2. Therefore, applying the forced first collision in the first scintillator (zone 1) it is possible to reduce the processing time by a factor of 2.

A fraction  $f_s$  of the incident neutrons is forced to collide in zone 1 and  $(1 - f_s)$  collide in zone 2. The counts in the proton-recoil spectrum become

$$X' = \begin{cases} X & \text{(scintillator 1),} \\ X \frac{f_s}{1 - f_s} (P/P_1 - 1) & \text{(scintillator 2),} \end{cases} \quad (7)$$

where

$$P = 1 - \exp(-\Sigma_T H_T)$$

and

$$P_1 = 1 - \exp(-\Sigma_T H_1).$$

The number of processed neutrons  $N'_s$  gives rise to a larger number of counts, given by

$$N'' = N'_s \frac{P}{P_1}. \quad (8)$$

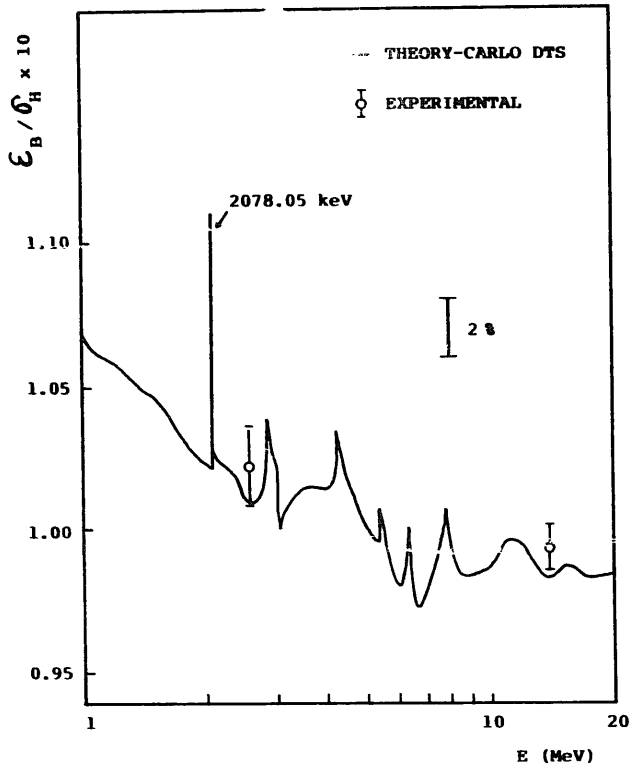


Fig. 2. DTS efficiency curve for 1 to 20 MeV neutrons. Spectrum bias at 30% of the maximum energy. The points at 2.446 and 14.04 MeV were obtained experimentally. The solid line is the Monte Carlo calculation.

The processing time is reduced by the factor  $N_s''/N_s'$ . The total reduction, including the forced collision with hydrogen becomes  $N_s''/N_s$ . At 14 MeV and using  $f_s = f_H = 0.9$ , the total reduction is 4.3.

5. Results of the calculations

5.1. DTS neutron detection efficiency

The behavior of the calculated biased efficiency with neutron energy is shown in fig. 2 together with two experimental points obtained at 2.446 and 14.04 MeV by means of the time correlated associated particle technique [1]. It can be seen that the experimental values agree with the calculated ones within the calculation error, which was around 0.8%. This error is much lower than reported previously (1.7%).

The following formula has been described previously for an easy calculation of the biased efficiency [1]:

$$\epsilon_B/\sigma_H = a_1 + a_2\sigma_c + a_3\sigma_H, \tag{9}$$

where  $\epsilon_B$  is the biased efficiency,  $\sigma_c$  is the carbon elastic plus inelastic scattering cross sections,  $\sigma_H$  is the  $H(n, n)H$  cross sections, and  $a_1, a_2, a_2$  are constants.

The values of  $a_1, a_2$  and  $a_3$  were obtained by a least-squares fit between the biased efficiency and the

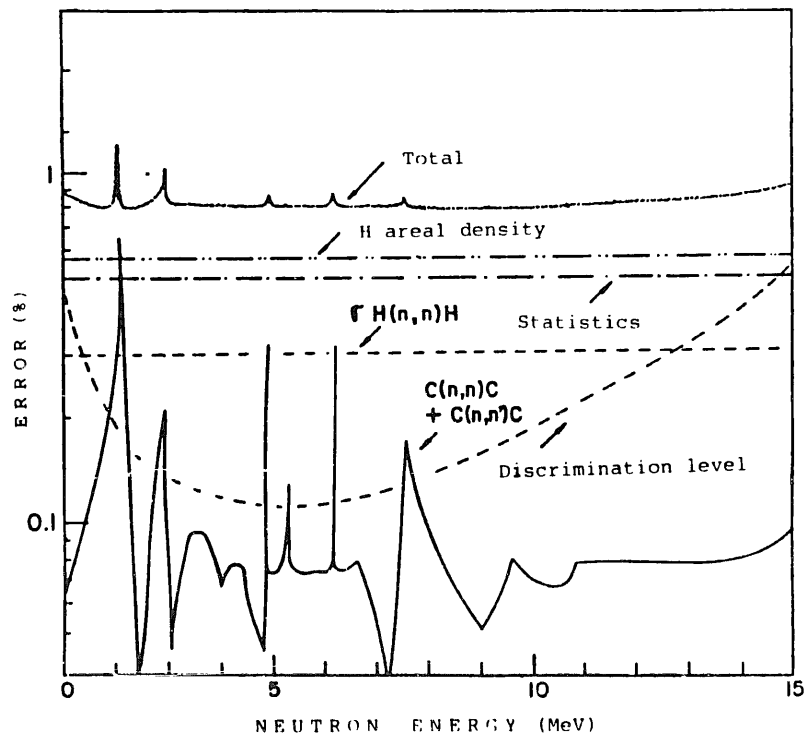


Fig. 3. Uncertainties in the CARLO DTS efficiency calculation.

Table 4  
Coefficients of the interpolation formula applicable to the DTS biased efficiency

Fractional bias energy	$a_1$ [ $\times 10^{-3}$ $b^{-1}$ ]	$a_2$ [ $\times 10^{-4}$ $b^{-2}$ ]	$a_3$ [ $\times 10^{-4}$ $b^{-2}$ ]	Reduced chi square
0.30	9.474	1.901	1.576	1.04
0.35	8.798	1.664	1.710	1.19
0.40	8.134	1.522	1.719	1.10

cross sections. Updated results of the fits are presented in table 4 for three fractional bias energies, namely: 0.30, 0.35 and 0.40 of the maximum energy. The average accuracy obtained in the interpolation goes from 0.8 to 1.8% at the fractional biases of 0.30 and 0.40, respectively. The updated values of these coefficients differ slightly from those published previously [1], due to the improvements performed in the code. In the new calculations the values of  $a_2$  are smaller, indicating less dependance on the carbon elastic and inelastic scattering.

The interpolation formula described above does not take into account variations in the efficiency caused by angular anisotropy in  $C(n, n)C$ ,  $H(n, n)H$  and  $^{12}C(n, n'\gamma)^{12}C$  reactions. For this reason, in applications where higher accuracy is desirable it is preferable to interpolate on parameter  $\epsilon_H/\sigma_H$ , as a function of the neutron energy. Moreover, the ENDF/B-VI data file should be used for the  $H(n, n)H$  cross section.

Fig. 3 shows the uncertainties involved in the calculated efficiency. The uncertainty indicated for the  $H(n, n)H$  cross section has been taken from ENDF/B-VI (0.3%). The predominant contributions to the total uncertainty are from the hydrogen areal density and statistics in the calculation, except near the carbon resonance at 2078 keV, where the multiple scattering uncertainty is predominant.

The uncertainty in the correction for lost coincidences has not been included in fig. 3 since it depends on the discrimination level used. This uncertainty is estimated to be around 10% of the correction (i.e. 0.4%) and has little contribution in the total uncertainty. The total uncertainty is between 0.8 and 1.0% except near the carbon resonance at 2078 keV, where it reaches the maximum value of 1.2%.

### 5.2. Proton recoil spectra

The comparison between the results of proton recoil spectra calculated by the code CARLO DTS and the experimental spectra obtained at 2.446 and 14.04 MeV has been shown in a previous paper [1]. The agreement between the new calculated and the experimental spectrum shapes remained excellent, indicating little sensitivity with respect to the selected bias energy.

## 6. Summary

A Monte Carlo code developed for the dual thin scintillator neutron detector efficiency and proton recoil spectrum calculation has been improved in order to obtain better accuracy and faster processing. Relativistic kinematics, anisotropy in the angular distributions and the forced collision technique were applied. The overall uncertainty in the calculated efficiency is between 0.8 and 1.0% in the 1–15 MeV range except near the carbon resonance at 2078 keV, where it reaches the maximum value of 1.2%. These values are substantially lower as compared to the previous ones [1]. The calculated and experimental efficiencies at two neutron energies, 2.446 and 14.04 MeV, agreed within the error in the calculated values, which is lower than reported previously. The agreement between the calculated and experimental spectrum shapes at these neutron energies remained excellent, indicating little sensitivity with respect to the selected bias energy.

## Acknowledgements

The author would like to thank the staff of the Neutron Interactions and Dosimetry group of the National Institute of Standards and Technology (NIST), USA for the support to the present work. He is specially indebted to Dr. Ronald G. Johnson for valuable discussions and for his calculation of the  $^{12}C(n, n')^3\alpha$  reaction  $Q$  values (table 2).

## References

- [1] M.S. Dias, R.G. Johnson and O.A. Wasson, Nucl. Instr. and Meth. 224 (1984) 532.
- [2] M.S. Dias, Ph.D. Thesis, University of São Paulo (1988), in Portuguese.
- [3] M.S. Dias, R.G. Johnson and O.A. Wasson. Proc. of an Advisory Group Meeting on Nuclear Standard Reference Data, Geel (1984), IAEA-TECDOC-335 (1985), p. 467.
- [4] J. Monahan, in: Fast Neutron Physics, Part I: Techniques, eds. J.B. Marion and J.L. Fowler (Interscience, New York, 1960) sect. 1. p. 49.
- [5] D.W. Glasgow, F.O. Purser, H. Hogue, J.C. Clement, K. Stelzer, G. Mack, J.R. Boyce, D.H. Epperson, S.G. Buccino, P.W. Lisowski, S.G. Glendinning, E.G. Bilpuch, H.W. Newson and C.R. Gould, Nucl. Sci. Eng. 61 (1976) 521.
- [6] ENDF/B-V, data file for  $^{12}C$ (MAT 1306), evaluation by C.Y. Fu and F.G. Perey (ORNL), BNL-NCS-17541 (ENDF-201), ed. R. Kinsey, available from the National Nuclear Data Center, Brookhaven National Laboratory, Upton, NY (July 1979).